Supplementary information

A combined method to quantify the retinal metabolic rate of oxygen using photoacoustic ophthalmoscopy and optical coherence tomography

Wei Song,[1,6,£] Qing Wei,[1,£] Wenzhong Liu,[1,£] Tan Liu,[1] Ji Yi,[1] Nader Sheibani,[2] Amani A. Fawzi,[3] Robert A. Linsenmeier,[1,3,4] Shuliang Jiao,[5] and Hao F. Zhang[1,3,*]

[1] Department of Biomedical Engineering, Northwestern University, Evanston, IL 60208, USA
[2] Department of Ophthalmology and Visual Sciences, University of Wisconsin, Madison, WI 53792, USA
[3] Department of Ophthalmology, Northwestern University, Chicago, IL 60611, USA
[4]Department of Neurobiology and Physiology, Northwestern University, Evanston, IL 60208, USA
[5]Department of Biomedical Engineering, Florida International University, Miami, FL 33174, USA
[6] Department of Physics, Harbin Institute of Technology, 92 West Da-Zhi Street Nangang District, Harbin, Heilongjiang 150080, China
[£] These authors contributed equally to the work presented here
[*]Corresponding author: hfzhang@northwestern.edu

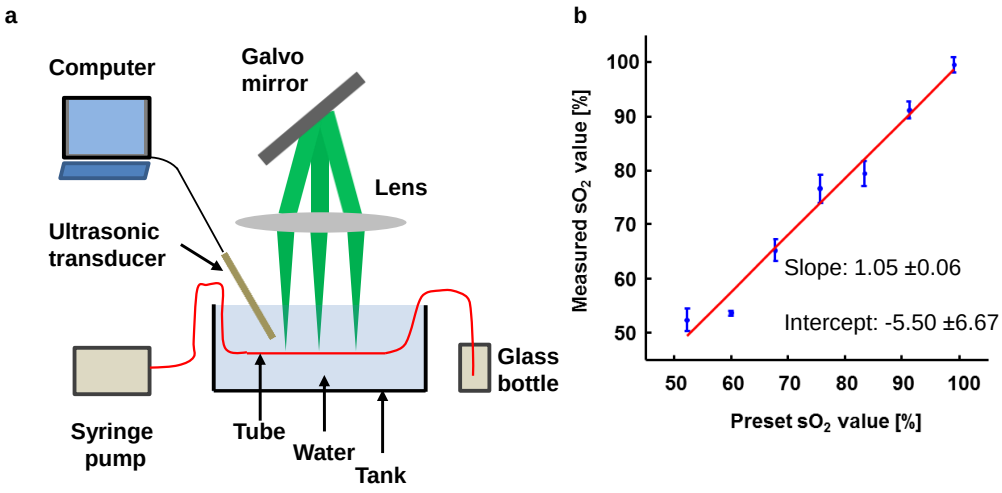

Supplementary Figure S1. (a) Experimental setup for blood phantom experiment; (b) comparison of sO_2 values measured by PAOM and a commercial blood analyzer.

We validated the accuracy of the PAOM system by measuring oxygen saturation (sO_2) values in a series of bovine blood phantom samples (Quad Five Inc.) with different preset sO_2 levels. We prepared the deoxygenated and oxygenated blood by respectively exposing the bovine blood to pure nitrogen gas and air for one hour. The prepared deoxygenated blood and oxygenated blood were then analyzed using a blood analyzer (Rapidlab, Siemens Inc.) Related blood parameters are listed in Supplementary Table S1. Such blood parameters were used to convert the oxygen partial pressure into sO_2 value based on Kelman equation[1]. The blood analyzer showed that sO_2 was 52.3% in deoxygenated blood and 99.1% in oxygenated blood. Several blood phantom samples at different sO_2 levels were created by mixing deoxygenated and oxygenated blood at different volumetric ratios.

Supplementary Table S1 Parameters of blood phantoms

Parameters	Oxygenated blood	Deoxygenated blood
PO_2(mmHg)	207.7	30.7
PCO_2(mmHg)	27.9	18.6
Temperature(^oC)	37	37
PH	7.16	7.27
sO_2 (%)	52.3	99.1

The experimental setup for blood phantom imaging is shown in Supplementary Figure S1a. The blood phantom samples were pumped (A-99, Razel) into a capillary tube (inner diameter: 250 μm; outer diameter: 500 μm; CTPS250-500, Paradigm Optics). The portion of the tube imaged by PAOM was placed in water for ultrasonic coupling. The illumination laser was weakly focused on the tube and the laser induced acoustic signals were collected by the same ultrasonic transducer (central frequency: 40-MHz; bandwidth: 30-MHz; active element size: 0.5×0.5 mm^2) as we used in our *in vivo* experiments. The PAOM measured sO_2 values are consistent with the independently measured sO_2 values by the blood analyzer as showed in Supplementary Figure S1b，a liner relationship between measured sO_2 and preset sO_2 was found to be: 1.05×(preset sO_2)-5.5=(measured sO_2) (r=0.98, r is the coefficient of determination). This blood phantom experiment confirmed the accuracy of the PAOM system in sO_2 quantification.

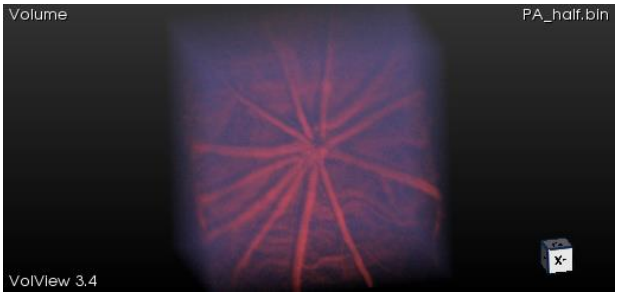

Supplementary Figure S2. A movie showing the three dimensional visualization of PAOM retinal image.

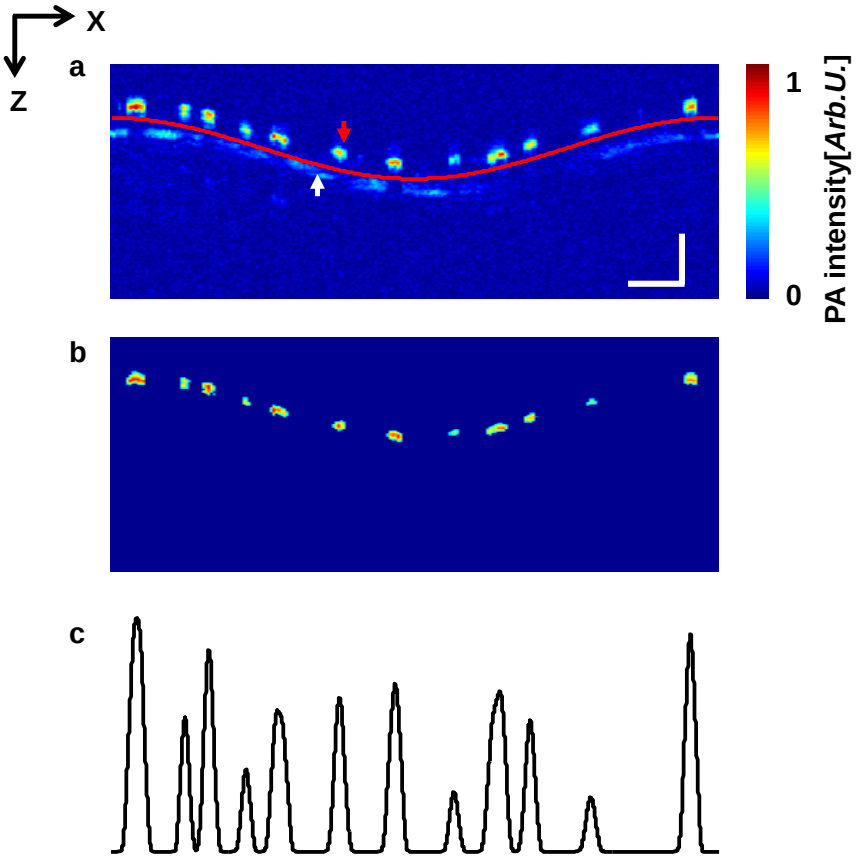

Supplementary Figure S3. Steps to extract photoacoustic signals from retinal vessels for sO_2 calculation. (a) Raw PAOM B-scan image. We can clearly observe both the retinal vessels (indicated by the red arrow) and choroidal vessels (indicated by the white arrow). In order to analyze the sO_2 within retinal vessels conveniently, we segmented retinal vessels out from the raw PAOM B-scan image by first fitting a curve (red line) between retinal and choroidal vessels, and then setting all pixel intensities to 0 beneath the fitted curve to remove choroidal vessel contributions. We filtered the B-scan image with a 5×5 median filter after segmentation to reduce background noise. (b) Demonstration of retinal vessels after segmentation and noise reduction. (c) Photoacoustic signal intensities from retinal vessels. We extracted the photoacoustic signals from retinal vessels through maximal amplitude projection along the *z*-axis. Bar: 250 μm.

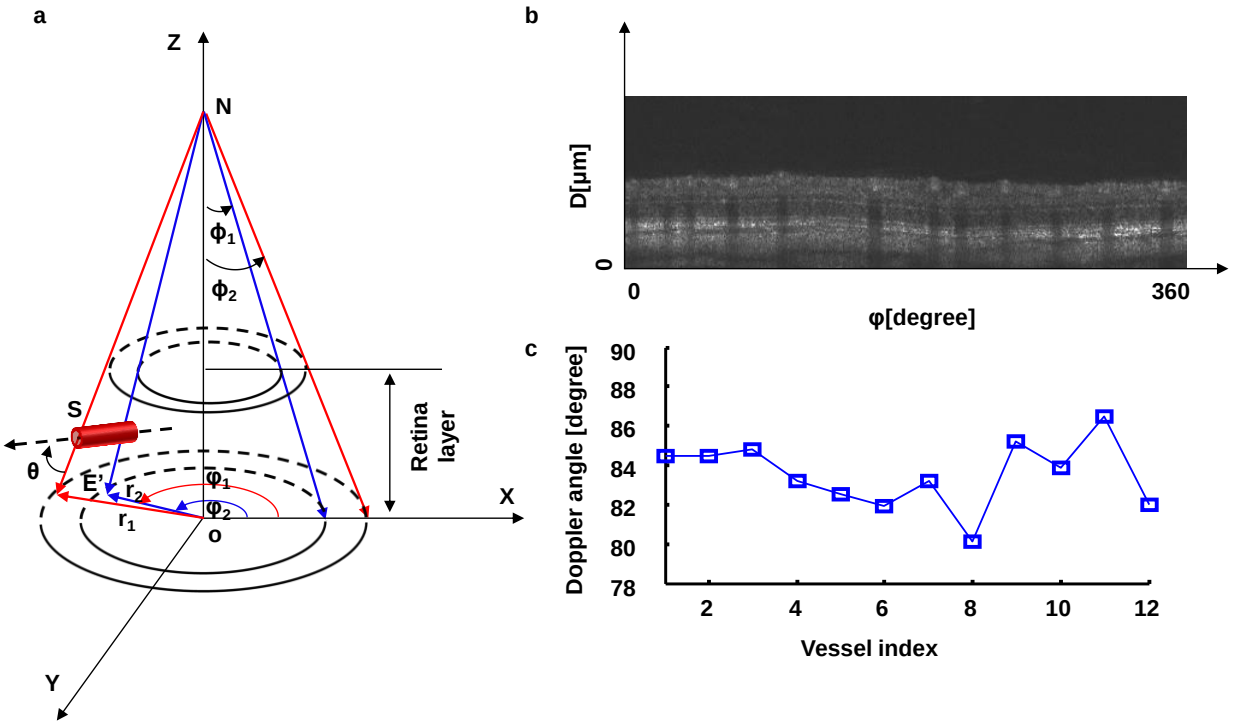

Supplementary Figure S4. Illustration of Doppler angle estimation in OCT using a dual-ring scan protocol. (a) Geometry of Doppler angle estimation based on dual-ring scan OCT. (b) A sample OCT amplitude image from inner circular B-scan. (c) Calculated Doppler angles along the inner circle.

In Doppler OCT, the Doppler angle (the angle between the vessel and the probing light) is required to measure absolute blood flow[2, 3]. Using the dual-ring scan protocol shown in Supplementary Figure S4a, the Doppler angle θ can be calculated as

$$\cos(\theta) = \frac{\overrightarrow{ES} \times \overrightarrow{NS}}{|\overrightarrow{ES}| \times |\overrightarrow{NS}|} \tag{S1}$$

where $\overrightarrow{ES}$ describes the direction of retinal vessel flow and $\overrightarrow{NS}$ gives the direction of the probing light. We can obtain $\overrightarrow{ES}$ and $\overrightarrow{NS}$ by determining the coordinates of *E*, *S* and *N*, where *E*, *S* represent the center points of the sample vessel in the inner and outer circular B-scan images and *N* is the nodal point of the eye. We can access the coordinates of *E*, *S* and *N* by obtaining vessel center positions within the circular B-scan image as shown in Supplementary Figure S4b. For generality, we assume that the sample vessel center positions within inner and outer circular B-scans are (φ_1, D_1) and (φ_2, D_2). We also assumed that the rat eyeball diameter is *h* without loss of

generality (the reported value is 6 mm[4]), which is the length of *NO*' and by extension of *NO* since the retina is very thin compared to the eyeball size. The coordinates of *E*, S and *N* are

$$E = (r_1 \times \cos(\varphi_1),\ r_1 \times \sin(\varphi_1),\ (D_1 + (r_1^2 + h^2)^{1/2} - h) \cdot \cos(\phi_1))$$
$$= (h \times \tan(\phi_1) \times \cos(\varphi_1), h \times \tan(\phi_1) \times \sin(\varphi_1), (D_1 + ((h \times \tan(\phi_1))^2 + h^2)^{1/2} - h) \cdot \cos(\phi_1)) \quad \text{(S2)}$$

$$S = (r_2 \times \cos(\varphi_2),\ r_2 \times \sin(\varphi_2),\ (D_2 + (r_2^2 + h^2)^{1/2} - h) \cdot \cos(\phi_2))$$
$$= (h \times \tan(\phi_2) \times \cos(\varphi_2), h \times \tan(\phi_2) \times \sin(\varphi_2), (D_2 + ((h \times \tan(\phi_2))^2 + h^2)^{1/2} - h) \cdot \cos(\phi_2)) \quad \text{(S3)}$$

$$N = (0,0,h) \quad \text{(S4)}$$

With these, the Doppler angle can then be calculated.

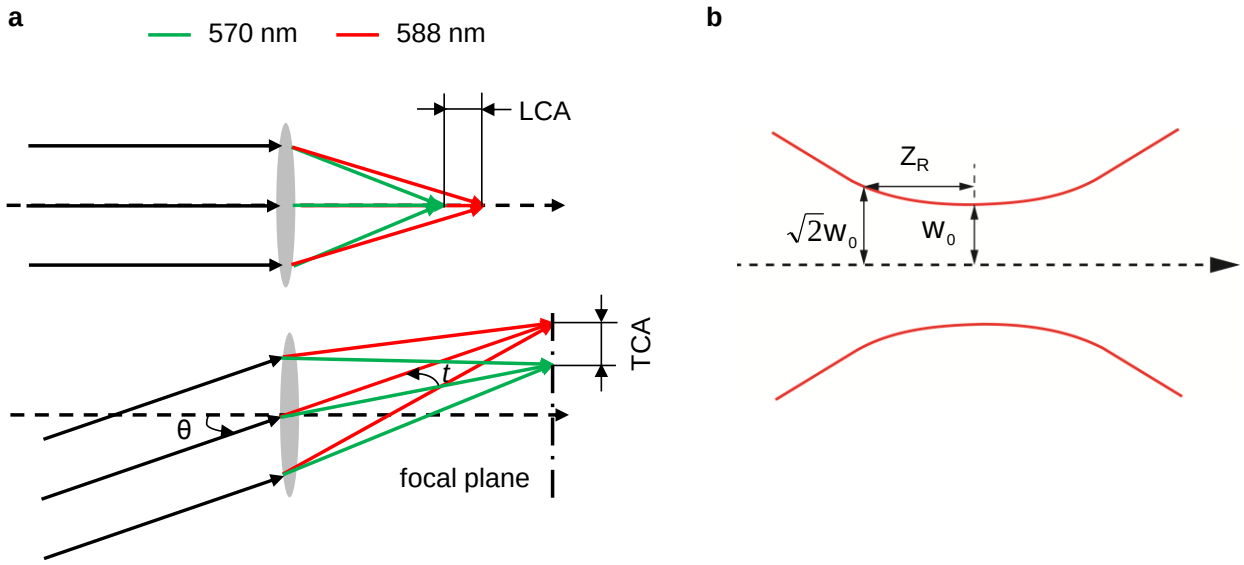

Supplementary Figure S5. Diagram of (a) Longitude chromatic aberration (LCA) and Transverse chromatic aberration (TCA) (b) Rayleigh length.

The reported chromatic power difference for a rat eye is 5.8 D from 486 nm to 656 nm[5]. In our current study, the optical window we used for sO_2 measurement was from 570 nm to 588 nm. We estimated the corresponding chromatic power difference within the optical window as:

$$\Delta P = \frac{5.8}{656-486} \cdot (588-570) = 0.61D \quad \text{(S5)}$$

Alternatively, the power difference can also be estimated as:

$$\Delta P = \frac{1}{f_{570}} - \frac{1}{f_{588}}, \quad \text{(S6)}$$

where f_{570} is the focal length of the rat eye lens at 570 nm; and f_{588} is the focal length at 588 nm. To make the analysis simple, we assume that f_{570} is 6 mm (the typical rat eyeball diameter) at 570 nm, which determines f_{588} to be 6.022 mm given the power difference is 0.61D. Thus, the longitudinal chromatic aberration (LCA) results in 22 μm focus shift from 570 nm to 588 nm.

The transverse chromatic aberration (TCA) causes the focal angle shift between different wavelengths, as demonstrated by *t* in Supplementary Figure S5a (bottom), where the *t* value is also related to the angle between optical axis of the rat eye and probing beam[6]. In our experiments, the maximum angle between the optical axis of the rat eye and the probing beam is 10 degrees. To our knowledge, the TCA values for the rat eye were not reported directly; yet it's estimated to be 5 to 10 times larger than the values of a human eye[7, 8]. The reported TCA for a human eye is characterized by the *t* value around 0.00325 degrees from 570 to 588 nm with an angle between optical axis and probing beam being 10 degrees. Assume the rat's *t* value is 10 times larger than a human's, then the *t* value for a rat is 0.0325 degree. With the typical rat eyeball size of 6 mm, such a *t* value as 0.0325 degree will lead to TCA value of 3.4 μm as showed in Supplementary Figure S5a.

Whether or not the LCA will affect PAOM imaging quality depends on the Rayleigh length Z_R of the probing beam that focuses on the retina, since within Z_R the optical fluence and lateral optical resolution were considered a relative constant. The focal spot of PAOM is estimated to be 20 μm, which gives Z_R (Supplementary Figure S5b) to be

$$Z_R = \frac{\pi \cdot 10^2}{588 \cdot 10^{-3}} = 534.3 \mu m \quad . \tag{S7}$$

Since the LCA value is much smaller than Z_R, we believe that the LCA will have little effect on sO_2 measurement in PAOM. Regarding the TCA, it can degrade the lateral optical resolution up to 3.4 μm at most, which is not expected to influence the sO_2 measurement very much because the TCA is much smaller (more than 4 times smaller) than the lateral resolution of the PAOM (20 μm)

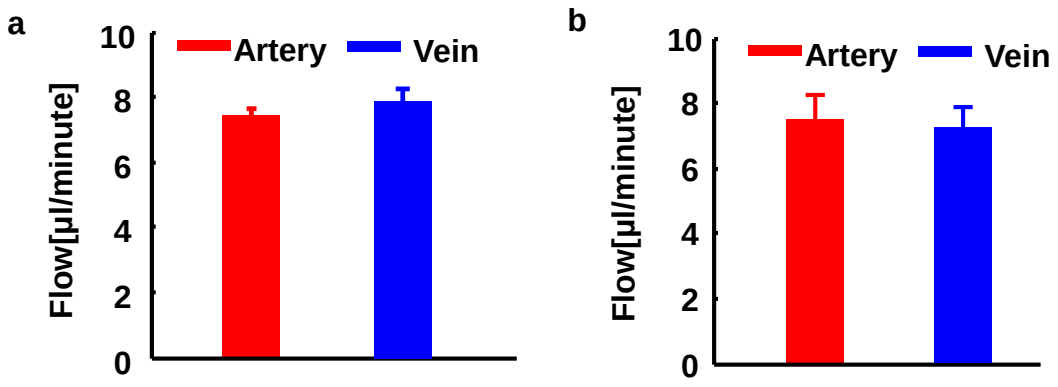

Supplementary Figure S6 Consistency of retinal absolute blood flow measured at (a) 70 kHz and (b) 25 kHz A-line rates.

In our dual-ring scan protocol, there are a total of 4096 A-lines in each circular B-scan, and we scanned 8 pairs of small-big rings consecutively. At the 70-kHz A-line rate, the time interval between two consecutive circular B-scans was 0.0585 s. At the 25-kHz A-line rate, the time interval between two consecutive B-scans was 0.1638 s. During experimentation, the heart rate was measured to be around 223 per minute, which means that the time interval between two successive heart beat was 0.269 s. Hence, 70-kHz is considered sufficiently high to sample the complete pulsatile profile flow, guaranteeing accurate flow estimations. In our studies, at the 70-kHz A-line rate, the measured retinal blood flows were 7.42±0.23 µl/minute (artery) and 7.78±0.38µl/minute (vein), as shown in Supplementary Figure S6a. At the 25-kHz A-line rate, the measured retinal blood flows were 7.49±0.73 µl/minute (artery) and 7.22±0.68 µl/minute (vein) as demonstrated in Supplementary Figure S6b, which agrees with the 70-kHz results. As a result, this study confirms that an accurate retinal blood flow assessment can be made at the 25-kHz A-line.

Supplementary Table S2. Summary of measured retinal vessel diameter, blood velocity, sO_2, and calculated blood flow.

Blood vessel	Diameter (μm)	Velocity (mm/s)	sO_2 (%)
1	47.7	10.1	94.6
2	48.9	-7.1	82.9
3	47.6	8.2	86.8
4	68.8	-7.7	77.7
5	54.3	8.5	94.2
6	70.4	-7.3	81.3
7	55.6	9.1	95.7
8	64.1	-5.6	84.7
9	64.9	10.5	95.5
10	62.6	-8.7	59.8
11	63.6	8.8	91.1
12	64.2	-7.8	77.1

Supplementary Note Laser safety evaluation

The allowable maximum permissible exposure (MPE) in PAOM using a repetitive-pulse laser is determined by wavelength, pulse repetition frequency, duration of a single pulse, and total duration of complete exposure. In our present study, these values are

Wavelength: 570, 578, 588 nm

Pulse repetition frequency: 25 kHz

Duration of single pulse: 5 ns

Duration of complete exposure during 8 pairs of dual-ring circular scanning: 2.6 s

The rat pupil size is 4 mm in diameter, which gives the area as 0.1257 cm^2

There are three testing rules for MPE:

Rule 1. Single pulse limit. The MPE is limited by the pulse width maximum energy in a pulse train (MPE_{SP}) for any single pulse during the exposure (assuming exposure to only one pulse)

$$MPE_{SP} = 5\times10^{-7}\ J/cm^2$$

For a 5 ns pulse duration,

$$MPE{:}E = 5\times10^{-7} / 5\times10^{-9}\ W/cm^2 = 100\ W/cm^2.$$

Rule 2. Average-power limit. The MPE is limited to the MPE for the duration of all pulse trains, T, divided by the number of pulses, n, during T, for all exposure duration up to T_{max}. Here, the duration of complete exposure is 2.6 s

$$T = 2.6\ s$$

$$n = 2.6\times25000 = 65000$$

The MPE for a 2.6-s total exposure time is (ANSI value)

$$MPE = 1.8\times2.6^{0.75}\times10^{-3}\ W/cm^2 = 3.686\times10^{-3}\ W/cm^2$$

Rule 3: Repetitive-pulse limit. The MPE is limited to MPE_{SP} multiplied by a correction factor C_P, *i.e.*, $n^{-0.25}$, where n is the number of pulses that occur during the exposure duration T_{max}.

$$C_P = n^{-1/4} = 65000^{-1/4} = 0.0626$$

$$MPE = 100\times0.0626\ W/cm^2 = 6.26\ W/cm^2$$

Based on above calculations, rule 2 dominates.

$DutyCycle = 5\times10^{-9}\times25\times10^{3} = 1.25\times10^{-4}$s

$E_{Pulse}\times n\times DutyCycle\ /2.6/0.1257\ cm^2 = 3.686\times10^{-3}\ W/cm^2$

$E_{Pulse} = 3.686\times10^{-3}/n/DutyCycle\times2.6\times0.1257 = 148.27\ \mu J$

In our experiments, the pulse energy we used is 40 nJ/ per pulse, which is within the ANSI laser safety limit.

References:

1. Kelman, G.R. Digital computer subroutine for the conversion of oxygen tension into saturation. *J. Appl. Physiol.* **21**, 1375-1376 (1966).
2. Wang, Y., Bower, B.A., Izatt, J.A., Tan, O. & Huang, D. Retinal blood flow measurement by circumpapillary Fourier domain Doppler optical coherence tomography. *J. Biomed. Opt.* **13**, 064003 (2008).
3. Wang, Y., Bower, B.A., Izatt, J.A., Tan, O. & Huang, D. In vivo total retinal blood flow measurement by Fourier domain Doppler optical coherence tomography. *J. Biomed. Opt.* **12**, 041215 (2007).
4. Hughes, A. A schematic eye for the rat. *Vision Res.* **19**, 569-588 (1979).
5. Chaudhuri, A., Hallett, P.E. & Parker, J.A. Aspheric curvatures, refractive indices and chromatic aberration for the rat eye. *Vision Res.* **23**, 1351-1363 (1983).
6. Ogboso, Y.U. & Bedell, H.E. Magnitude of lateral chromatic aberration across the retina of the human eye. *J. Opt. Soc. Am. A* **4**, 1666-1672 (1987).
7. Remtulla, S. & Hallett, P.E. A schematic eye for the mouse, and comparisons with the rat. *Vision Res.* **25**, 21-31 (1985).
8. Harmening, W.M., Tiruveedhula, P., Roorda, A. & Sincich, L.C. Measurement and correction of transverse chromatic offsets for multi-wavelength retinal microscopy in the living eye. *Biomed Opt Express* **3**, 2066-2077 (2012).